Matter and Radiation at Extremes | RESEARCH ARTICLE | scitation.org/journal/mre

Analysis of electromagnetic pulses generation from laser coupling with polymer targets: Effect of metal content in target

Cite as: Matter Radiat. Extremes 5, 017401 (2020); doi: 10.1063/1.5114663
Submitted: 11 June 2019 • Accepted: 7 November 2019 •
Published Online: 27 December 2019

Yadong Xia,[1,2] Feng Zhang,[3] Hongbo Cai,[4,5,6] Weimin Zhou,[3] Chao Tian,[3] Bo Zhang,[3] Dongxiao Liu,[3] Tao Yi,[2] Yilin Xu,[1] Feng Wang,[2,a)] Tingshuai Li,[1,a)] and Shaoping Zhu[3,4,7]

AFFILIATIONS

[1]School of Materials and Energy, University of Electronic Science and Technology of China, Chengdu 611731, People's Republic of China
[2]Laser Fusion Research Center, China Academy of Engineering Physics, Mianyang 621900, People's Republic of China
[3]Science and Technology on Plasma Physics Laboratory, Laser Fusion Research Center, China Academy of Engineering Physics, Mianyang 621900, People's Republic of China
[4]Institute of Applied Physics and Computational Mathematics, Beijing, 100094, People's Republic of China
[5]HEDPS, Center for Applied Physics and Technology, Peking University, Beijing 100871, People's Republic of China
[6]IFSA Collaborative Innovation Center, Shanghai Jiao Tong University, Shanghai 200240, People's Republic of China
[7]Graduate School, China Academy of Engineering Physics, P.O. Box 2101, Beijing 100088, People's Republic of China

[a)]**Authors to whom correspondence should be addressed:** wangfeng7566@163.com and litingshuai@uestc.edu.cn

ABSTRACT

Powerful lasers interacting with solid targets can generate intense electromagnetic pulses (EMPs). In this study, EMPs produced by a pulsed laser (1 ps, 100 J) shooting at CH targets doped with different titanium (Ti) contents at the XG-III laser facility are measured and analyzed. The results demonstrate that the intensity of EMPs first increases with Ti doping content from 1% to 7% and then decreases. The electron spectra show that EMP emission is closely related to the hot electrons ejected from the target surface, which is confirmed by an analysis based on the target–holder–ground equivalent antenna model. The conclusions of this study provide a new approach to achieve tunable EMP radiation by adjusting the metal content of solid targets, and will also help in understanding the mechanism of EMP generation and ejection of hot electrons during laser coupling with targets.

I. INTRODUCTION

Inertial confinement fusion (ICF) has attracted enormous attention owing to its potential as a green energy source and its use for investigating physical processes under extreme conditions.[1,2] It has been shown that interaction of a high-intensity laser pulse with a target is critical for achieving ICF[2,3] together with the production of a large amount of X-rays,[4–7] plasmas,[8,9] and energetic electrons.[10,11] However, this process is also accompanied by the generation of high-intensity (>several hundreds of kiloelectronvolt per meter),[12,13] wideband (tens of megahertz–5 GHz) electromagnetic pulses (EMPs),[14–18] which not only reduce the accuracy of experimental data collection, but can also result in malfunction of diagnostic equipment.[16,19,20]

It has been found that plasmas produced by the laser–matter interaction are responsible for the generation of X-rays, electrons, and ions, while EMPs stem mainly from energetic hot electrons escaping from the target. A target charging model involving the ejection of an electron bunch from the target was established to analyze the physical process underlying EMP generation.[17,18,21] To confirm that emitted electrons were indeed the main source of EMPs, experiments were performed at the Lawrence Livermore National Laboratory (LLNL) in which the relationship between the EMP intensity and the energy of the emitted electrons was studied by changing the size of spherical or flat targets in the Titan laser facility.[16,22] The results indicated that the EMP intensity and the number of high-energy electrons increased

simultaneously with increasing target size. Identical results were obtained at the Rutherford Laboratory.[23] Moreover, the mechanisms of electron transport and electromagnetic radiation during laser interaction with Al and CH targets of different thicknesses were also investigated, and the effects of the emitted electrons on EMP generation were analyzed.[24] However, the relationship between transient electrons and EMPs generated by laser coupling with polymer targets doped with different metal contents has remained unexplored to date, although this is crucial for a deep understanding of the mechanism of EMP generation.

In this study, EMPs and hot electrons induced by a picosecond pulsed laser shooting at polymer targets doped with different titanium (Ti) contents at the XG-III laser facility are recorded by B-dot probes and an electron spectrometer, respectively. The relationship between EMP radiation and electron ejection is discussed in terms of a target–holder–ground radiating antenna model. It is found that the EMP intensity is closely related to the metal content of the polymer targets. The distribution of EMPs is also discussed. The resulting conclusions are significant for a thorough understanding of the physical processes related to electromagnetic radiation and electrons emitted from laser–plasma interaction, as well as for providing guidance with regard to improvements in potential applications of strong EMPs, such as electromagnetic pulse weapons,[25,26] mineral extraction,[27] and material forming technology.[28]

II. EXPERIMENTAL ARRANGEMENT

The measurements of EMPs are conducted at the XG-III laser facility at the Science and Technology on Plasma Physics Laboratory of the China Academy of Engineering Physics, which is based on a Ti-doped sapphire laser. XG-III adopts standard chirp pulse amplification (CPA) technology and can synchronously output three pulse widths in the nanosecond, picosecond, and femtosecond ranges, and three wavelengths of 527 nm, 1053 nm, and 800 nm. Our experimental layout is shown in Fig. 1, where a pulsed laser (1 ps, 100 J) is used, with a prepulse-to-main-pulse intensity contrast ratio of 3.5×10^{-7}. The laser is vertically incident onto the front surface of the polymer target (1000 μm × 1500 μm×200 μm), which has a minimum focal spot diameter of ~50 μm, and the corresponding intensity is up to 10^{18} W/cm^2. The CH polymer targets are doped with different Ti contents of 1%, 3%, 7%, and 12%. A magnetic field B-dot antenna and an electric field discone antenna[12,13] are mounted at 70° (position a) or 25° (position b) away from the laser beam, both at distances of 30 cm from the target. An electron spectrometer is installed at 0° (position c) or 20° (position d) to record the quantity and energy of electrons emitting from the back of the target. An electric field horn antenna is placed at 70° away from the laser beam, at a distance of 20 cm from the target chamber wall. The antennas, electron spectrometer, and targets are calibrated in the same plane.

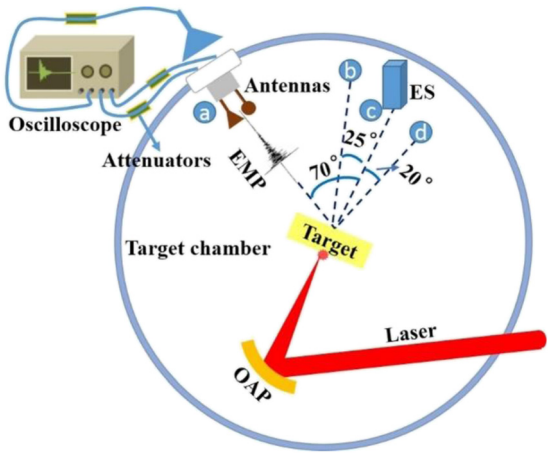

FIG. 1. Schematic of experimental arrangement.

The electromagnetic field signals are collected using a shielded oscilloscope (Tektronix, 12.5 GHz). Because of the great strength of the EMP signals, multiple attenuators are connected to the oscilloscope to protect it and to ensure accurate measurement of the signals.

The electron spectrometer, with a deflecting magnetic field of 4000 G, is calibrated before it is used for monitoring the ejected electrons, and an image plate (IP) is used to record the deflection distance of electrons, which can quantify electrons with different energy.

III. RESULTS AND DISCUSSION

For targets with different Ti doping contents (1%, 3%, 7%, and 12%), Fig. 2(a) shows time-domain waveforms of EMPs measured by the ultra-wideband (0.01–12 GHz) discone antenna at position a, while Fig. 2(b) shows the maximum, minimum, and average values of the EMP amplitudes.

The EMP waveforms clearly change as the Ti doping content varies from 1% to 12% in the solid CH target. The corresponding maximum amplitude values of EMPs are 832.78 V, 1104.51 V, 1504.16 V, and 1232.15 V [Fig. 2(a)], and the corresponding average values are 812.12 V, 1184.27 V, 1434.19 V and 1240.38 V [Fig. 2(b)], indicating that the EMP intensity first increases and then decreases with increasing Ti content in the CH target. The greatest amount of EMP radiation is obtained for the target doped with 7% Ti (1.8 times as much radiation as for 1% Ti). Before the arrival of the main laser (the 0 ns point), all EMP signals have a period of about 12 ns, which can be attributed to prepulse ablation, and the EMPs last for about 200 ns before they finally decay to noise (about 80 V). Thus, the EMPs observed in our experiment are of high intensity and also of long duration. To obtain more information about these EMP signals, the spectra of EMPs in the time domain are subjected to fast Fourier transformation (FFT), and the amplitudes of the spectra are then squared to give the power density spectra for different amounts of doping, as shown in Fig. 3(a).

It can be seen that EMPs inside the target chamber have broad frequency bands from 0 GHz to 1.6 GHz, with six typical peaks appearing at 180 MHz, 302 MHz, 815 MHz, 1.03 GHz, 1.21 GHz, and 1.43 GHz, and more peaks emerging between 1.03 GHz and 1.43 GHz. Many previous reports of EMP radiation have also suggested the presence of multiple peaks in the spectra.[29–31]

In this study, the typical frequency peaks can be attributed to three factors apart from noise. The first of these is the eigenfrequency radiation, which depends on the structure of the cylindrical target chamber, which has bottom radius R = 1.1 m and height l = 1.3 m. Cylindrical resonators have three typical resonant modes: TE_{111}, TM_{010},[32] and TE_{011}.[33] In the case of the TE_{111} mode, the resonant frequency f_r for this cavity can be expressed as[32]

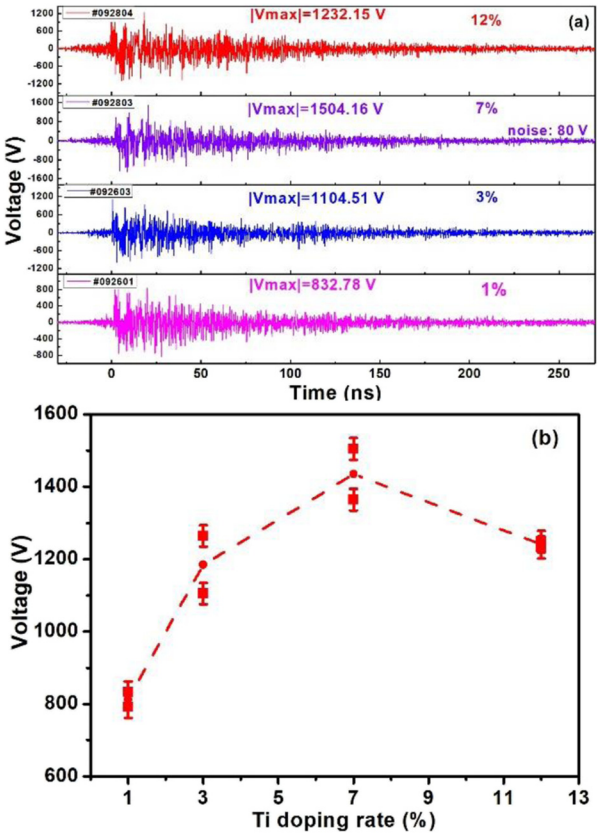

FIG. 2. (a) Time-domain waveforms of EMPs measured by the electric field discone antenna at position a for targets with different Ti doping contents. (b) Maximum, minimum, and average (dashed line) values of the EMP amplitude for targets with different Ti doping contents.

$$f_r = \frac{1}{2\pi\eta}\sqrt{\left(\frac{\mu_{11}}{R}\right)^2 + \left(\frac{\pi}{l}\right)^2}, \tag{1}$$

where $\eta = \sqrt{\mu/\varepsilon}$, μ and ε are the permeability and conductivity, respectively, of the gaseous medium in the resonant cavity, and $\mu_{11} = 1.841$ is the first root of the first-order Bessel function. The gaseous medium in the target chamber is at a pressure of just 5×10^{-2} Pa and so can be assumed to be in a vacuum state, so $\sqrt{\mu\varepsilon} = 1/c$ and $\eta = \frac{1}{c}$, where $c = 3 \times 10^8$ m/s is the propagation speed of electromagnetic waves in vacuum. Equation (1) can be approximated as

$$f_r \cong c\sqrt{(1/3.41R)^2 + (1/2l)^2}, \tag{2}$$

Therefore, the resonant frequency of the target chamber in this mode is 140.4 MHz.

In the case of the TM_{010} mode, the resonant frequency can be described as[32]

$$f_r = \frac{\nu_{01}}{2\pi R\sqrt{\mu\varepsilon}}, \tag{3}$$

where $\nu_{01} = 2.405$ is the first root of the zero-order Bessel function. After simplifying, we have

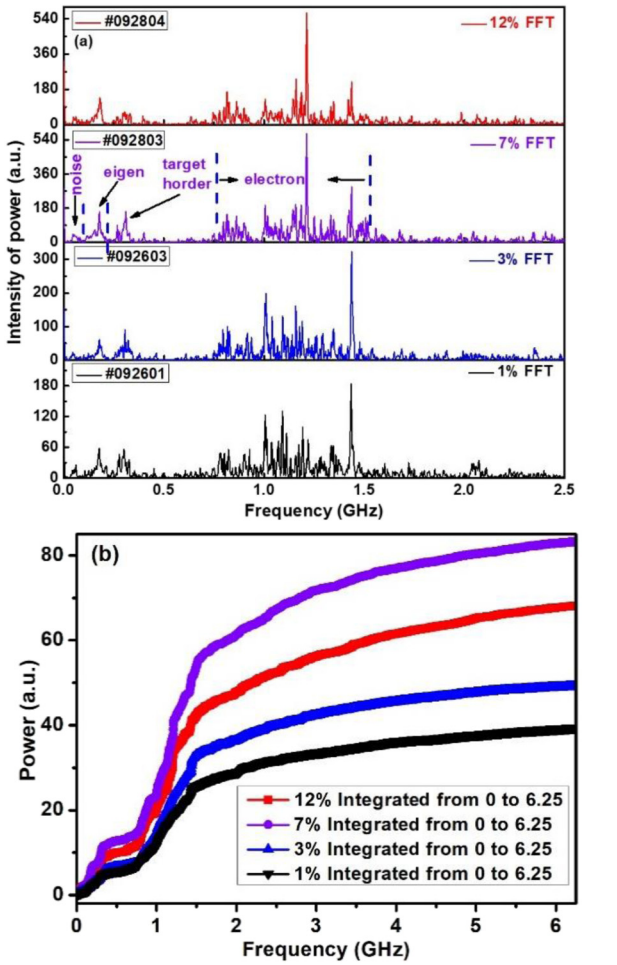

FIG. 3. (a) Power density spectra (the main portion from 0 Hz to 2.5 GHz) of EMPs obtained by FFT and squaring of the time-domain signals. (b) Integrated power density spectra of EMPs from 0 Hz to 6.25 GHz.

$$f_r \cong \frac{c}{2.62R}. \tag{4}$$

The resonant frequency of the chamber in this mode can be calculated as 104.9 MHz.

In the case of the TE_{011} mode, the simplified expression for the cavity resonant frequency is[33]

$$f_r \cong c\sqrt{(1/1.64R)^2 + (1/2l)^2}, \tag{5}$$

and the resonant frequency of the chamber is 202.4 MHz in this mode. Thus, the eigenfrequencies have been calculated from 100 MHz to 210 MHz.

The second typical frequency can be attributed to the metal target holder fixed on the chamber ground, with the target holder acting as a dipole antenna and the chamber ground as a mirror.[11] The emission frequency is given approximately by $f_a = \frac{c}{4l_h}$, where l_h is the length of the target holder. In this experiment, $l_h = 26$ cm, so $f_a = 289$ MHz.

The third typical frequency is attributed to the emitted hot electrons and is in the range from 0.7 GHz to 1.6 GHz.

The power density spectra from Fig. 3(a) are integrated from 0 GHz to 6.25 GHz, and the resulting total powers are shown in Fig. 3(b). The total powers (in arbitrary units) are 39.37, 49.04, 83.22, and 68.07 for 1%, 3%, 7%, and 12% Ti doping, respectively, which are consistent with the trend of the EMPs in the time domain.

The power density spectra of EMPs measured by the horn antenna outside the target chamber are displayed in Fig. 4(a). It is clear that the EMPs outside the chamber have frequency domains from 0.4 GHz to 1.6 GHz, with typical peaks being observed at 0.41 GHz, 0.55 GHz, 0.8 GHz, 1.48 GHz, and 1.74 GHz, and that the intensities are remarkably weaker than those inside the chamber. It should also be noted that the eigenfrequency radiation[32,33] and target holder frequency radiation disappear, but EMPs generated by the escaping hot electrons still exist. This is mainly because the eigenfrequency radiation and electromagnetic radiation from the target holder depend on the internal structure of the target chamber. However, the EMPs outside the target chamber are only slightly affected by the cavity structure, so EMPs in the eigenfrequency and target holder frequency ranges are weakened after penetrating the wall of the chamber. In addition, since the half-wavelengths of EMPs with frequencies of 0.5 GHz and 0.6 GHz are 30 cm and 25 cm, respectively, and since the distance between the horn antenna and the target chamber wall is 20 cm and the depth between the middle of the horn antenna and the horn mouth is 9 cm, a half-wavelength resonance will occur between the target chamber wall and the horn antenna, resulting in much stronger EMP emissions in this frequency band.

The power spectra outside the target chamber are integrated for different doping ratios, and the resulting total radiant power of EMPs is given in Fig. 4(b), where values (in arbitrary units) of 0.11, 0.15, 0.38, and 0.36 are obtained for 1%, 3%, 7% and 12% Ti doping, respectively, which are much weaker than those inside the chamber, indicating that EMPs undergo more than 200-fold attenuation after passing through the target chamber wall. Figure 5 shows EMPs from the shots with 3% Ti doped targets in the target chamber. The EMP (lasting 50 ns) at 25° is 1.6 times stronger and survives longer than that at 70°, which can be attributed to more hot electrons being produced at the location closer to the laser propagation direction,[34,35] confirming that stronger and wider-band EMPs are generated at 25° than at 70°. Moreover, it is found that the EMP durations measured by the magnetic field B-dot detector are shorter than those measured by the electric field discone antenna, which is mainly because the B-dot detector only receives EMPs from its front, since its other side is shielded, thus excluding reflected waves.

When the laser power density exceeds 10^5 W/cm^2, the electric field of the laser is sufficient to overcome the Coulomb field in some atoms to allow direct extraction of electrons from these atoms, and the state can be basically considered as a plasma.[36] Subsequently, the laser energy is deposited in the plasma region through multiple mechanisms, including resonant absorption,[37] vacuum heating,[38] and $\mathbf{J} \times \mathbf{B}$ heating,[39] thereby generating super-high-temperature electrons. In our experiment, the intensity of the laser reaches 10^{18} W/cm^2, and when the targets are irradiated by femtosecond pulses, EMPs and hot

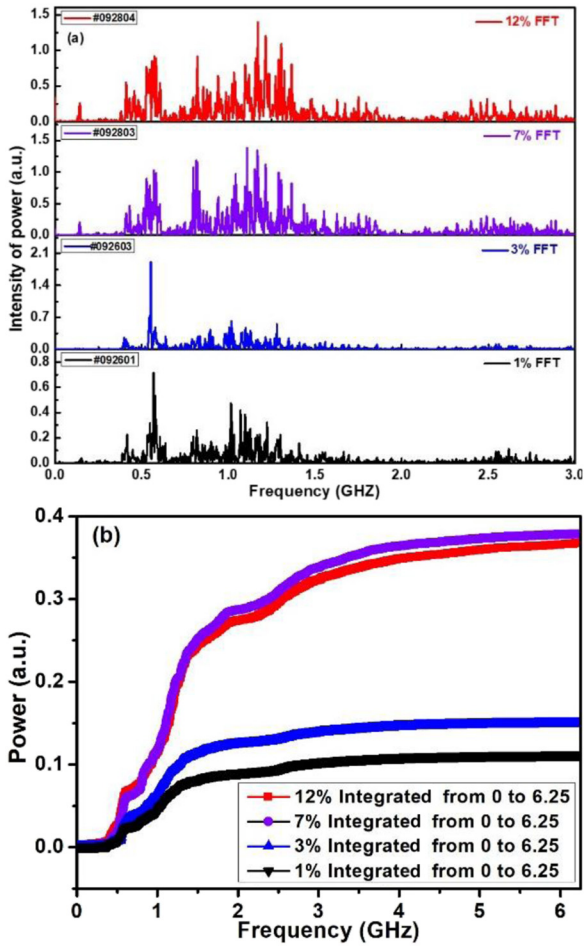

FIG. 4. (a) Power density spectra of EMPs measured by the horn antenna outside the target chamber (the main portion from 0 Hz to 3 GHz). (b) Integrated power density spectra of EMPs from 0 Hz to 6.25 GHz.

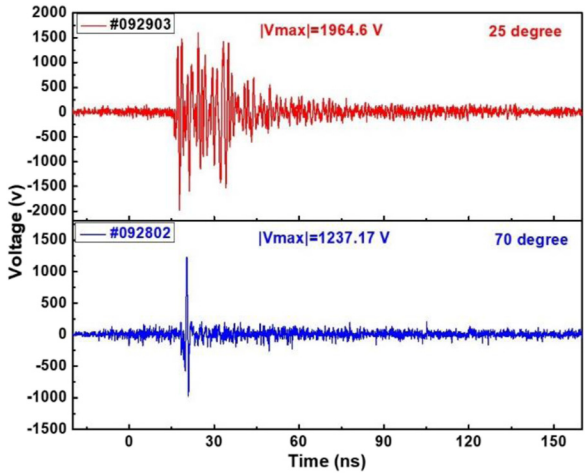

FIG. 5. EMP signals measured by a magnetic field B-dot antenna at positions a (70°) and b (25°) for the shots with 3% Ti doped targets.

electrons are found to be generated simultaneously. To reveal the relationship between them, the hot electrons escaping from the plasma are recorded by the electron spectrometer installed at 0° or 20°.

Figure 6 displays the evolution of the electron energy spectra of a 7% Ti doped target, and the values of the energy spectra from 0.32 MeV to 20 MeV are integrated to describe the hot electric quantum yield per unit solid angle. In Fig. 6(a), the number of hot electrons ejected from the plasma first increases to a peak value and then decreases, with a high energy of up to 20 MeV at 0° and an energy of 14 MeV at 20°, and with the peak values of both energy spectra being about 2.21 MeV. In Fig. 6(b), the total number of electrons per solid angle is 1.07×10^{11}/sr at 0°, which is 1.41 times as many as at 20°, 7.58×10^{10}/sr. These results indicate that more hot electrons with higher energies escape from the plasma in the laser propagation direction.

It has been reported that the absorption efficiency of lasers in metal targets is larger than that in nonmetal targets, and that the total number of hot electrons ejected from metal targets is greater than that from nonmetal targets,[40] which can be accounted for by the ability of metals to produce more free electrons to neutralize charges from the target. Therefore, a small amount of metal content in a CH target will affect the number and energy of the electrons escaping from the plasma.

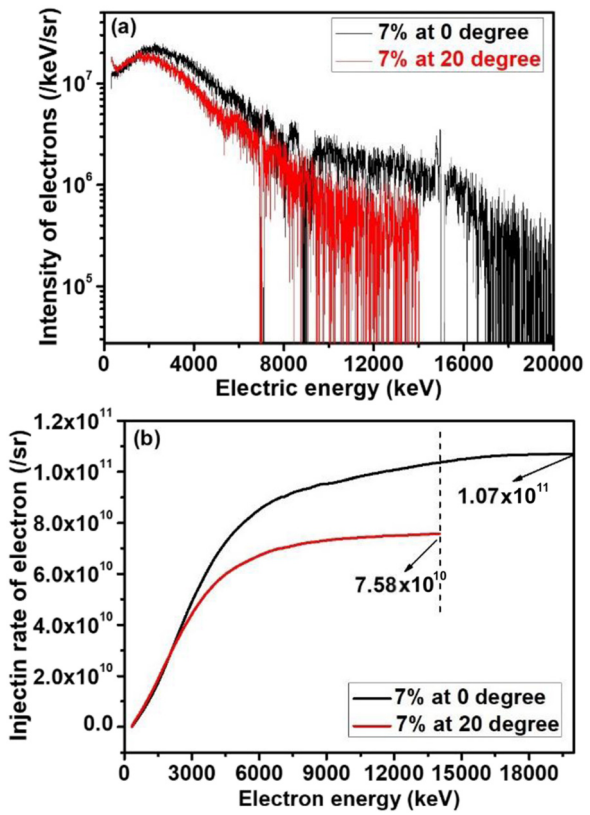

FIG. 6. (a) Original hot electron energy spectra for a 7% doped target at 0° and 20°, where 0° is the laser incidence direction and the black and red lines are for 0° and 20°, respectively. (b) Integrated spectra from (a).

According to the target–holder system model,[11] the process of multiple reflux and ejection of hot electrons will induce EMPs with varying intensities and frequencies, and the total quantity of charge of electrons that are able to break through the potential barrier can be expressed as

$$Q = eN_e \int_{T_h \Delta\widehat{\phi}_{\rm th}}^{\infty} f_e(\varepsilon_e) d\varepsilon_e, \tag{6}$$

where e is the electron charge, T_h the thermionic temperature, $\phi_{\rm th}$ the potential, N_e the total number of hot electrons, ε_e the hot-electron energy, $\Delta\widehat{\phi}_{\rm th}$ the potential barrier, and $f_e(\varepsilon_e)$ the hot electron distribution.

Figure 6(a) presents the number of escaping electrons that have overcome the potential barrier $\Delta\widehat{\phi}_{\rm th}$ at 0° and 20°. The divergence angle is 40° (HWHM), which is equivalent to 1.6 sr. Therefore, $N_e = 1.22 \times 10^{11}$ according to a linear fitting estimate. The quantity of charge can be estimated as $Q \cong eN_e$, and $I_e \cong Q/t_{\rm las}$.[11] In this experiment, $t_{\rm las} = 1$ ps, and Q is thus calculated to be 1.95×10^{-8} C and I_e to be 1.95×10^4 A.

The intensity of the radiated electromagnetic field in the target–holder–ground dipole model illustrated in Fig. 7 is given by

$$B_e = \frac{\mu_0 I_e \cos\left(\frac{1}{2}\pi \cos\theta\right)}{2\pi D \sin\theta}, \tag{7}$$

where $\mu_0 = 4\pi \times 10^{-7}$ T m/A is the permeability of the vacuum, B_e the electric field intensity, D the distance between the B-dot antenna and the center of the ground, and θ the angle from the B-dot antenna to the dipole antenna axis, as shown in Fig. 7. In this case, since $D = 39.7$ cm and $\theta = 49.1°$, B_e is estimated as 1.303×10^{-2} T. According to Faraday's law of electromagnetic induction,

$$V = -\frac{d\varphi}{dt}, \tag{8}$$

$$\varphi = BS, \tag{9}$$

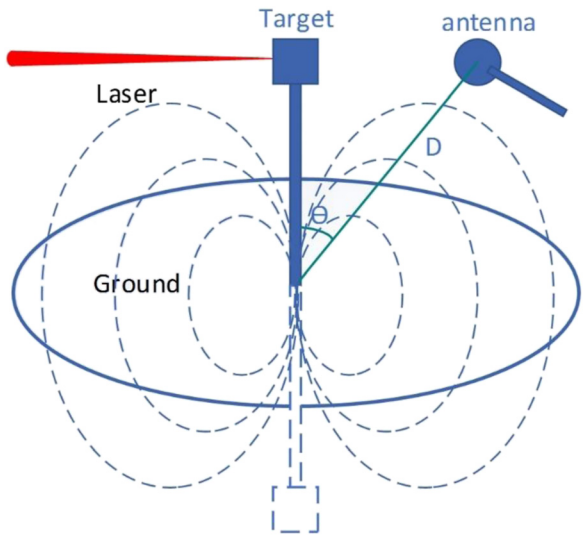

FIG. 7. Target–holder–ground dipole radiation model.[11]

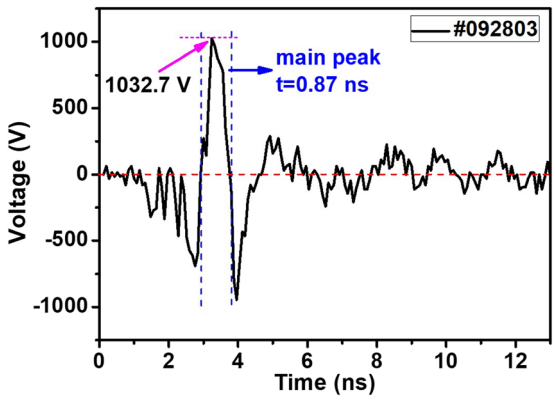

FIG. 8. EMP signal measured by a magnetic field B-dot antenna (at position a) for a 7% Ti doped target.

where V is the voltage generated by electromagnetic induction, φ the magnetic flux, $B = B_e$ the magnetic induction intensity, and t the time at which the magnetic flux passes the B-dot. In Fig. 8, it can be seen that the duration of the main peak is 0.87 ns, and so we can take $t = 0.87$ ns, and $S = 7.85 \times 10^{-5}$ m^2 is the equivalent area of the B-dot antenna. The absolute voltage of induction is calculated to be 1175 V, which is decreased in the actual experiment owing to attenuation in the cable and to ambient noise (about 80 V). Therefore, the simulated result is in good agreement with the magnetic field signal voltage of the electromagnetic pulse of 1032.7 V, as shown in Fig. 8, confirming that EMPs can be attributed to hot electrons ejected from the plasma.

IV. CONCLUSION

The characteristics of EMPs generated by the interaction between a picosecond laser and polymer targets doped with different Ti contents have been analyzed. The EMPs have broad frequency bands from several megahertz to 1.6 GHz, and the energy of EMPs outside the target chamber is degraded 200-fold compared with that of EMPs inside the chamber. The EMP intensity first increases and then decreases with increasing Ti doping content, with the peak intensity being observed for the target doped with 7% Ti. An analysis based on a target–holder–ground equivalent antenna model has shown that the EMPs originate from emitted hot electrons.

ACKNOWLEDGMENTS

We would like to thank the Science and Technology on Plasma Physics Laboratory of the China Academy of Engineering Physics for their kind help with the experiment. This work is supported by the Science Challenge Project (No. TZ2016005).

REFERENCES

[1]E. M. Campbell, V. N. Goncharov, T. C. Sangster, S. P. Regan, P. B. Radha, R. Betti, J. F. Myatt, D. H. Froula, M. J. Rosenberg, I. V. Igumenshchev, W. Seka, A. A. Solodov, A. V. Maximov, J. A. Marozas, T. J. B. Collins, D. Turnbull, F. J. Marshall, A. Shvydky, J. P. Knauer, R. L. McCrory, A. B. Sefkow, M. Hohenberger, P. A. Michel, T. Chapman, L. Masse, C. Goyon, S. Ross, J. W. Bates, M. Karasik, J. Oh, J. Weaver, A. J. Schmitt, K. Obenschain, S. P. Obenschain, S. Reyes, and B. Van Wonterghem, "Laser-direct-drive program: Promise, challenge, and path forward," Matter Radiat. Extremes **2**, 37 (2017).

[2]S. Kawata, T. Karino, and A. I. Ogoyski, "Review of heavy-ion inertial fusion physics," Matter Radiat. Extremes **1**, 89–113 (2016).

[3]F. Consoli, R. D. Angelis, L. Duvillaret, P. L. Andreoli, M. Cipriani, G. Cristofari, G. G. Di, F. Ingenito, and C. Verona, "Time-resolved absolute measurements by electro-optic effect of giant electromagnetic pulses due to laser-plasma interaction in nanosecond regime," Sci. Rep. **6**, 27889 (2016).

[4]A. S. Sandhu, G. R. Kumar, S. Sengupta, A. Das, and P. K. Kaw, "Laser-pulse-induced second-harmonic and hard x-ray emission: Role of plasma-wave breaking," Phys. Rev. Lett. **95**, 025005 (2005).

[5]M. Anand, S. Kahaly, G. Ravindra Kumar, M. Krishnamurthy, A. S. Sandhu, and P. Gibbon, "Enhanced hard x-ray emission from microdroplet preplasma," Appl. Phys. Lett. **88**, 181111 (2006).

[6]K. H. Liao, A. G. Mordovanakis, B. Hou, G. Chang, M. Rever, G. A. Mourou, J. Nees, and A. Galvanauskas, "Generation of hard X-rays using an ultrafast fiber laser system," Opt. Express **15**, 13942–13948 (2007).

[7]A. L. Kritcher, T. Döppner, C. Fortmann, O. L. Landen, R. Wallace, and S. H. Glenzer, "Development of X-ray Thomson scattering for implosion target characterization," High Energy Density Phys. **7**, 271–276 (2011).

[8]I. I. Beilis, "Mechanism of laser plasma production and of plasma interaction with a target," Appl. Phys. Lett. **89**, 091503 (2006).

[9]M. M. Murnane, H. C. Kapteyn, and R. W. Falcone, "Generation of efficient ultrafast laser-plasma x-ray sources," Phys. Fluids B **3**, 2409–2413 (1991).

[10]H. B. Zhuo, Z. L. Chen, Z. M. Sheng, M. Chen, T. Yabuuchi, M. Tampo, M. Y. Yu, X. H. Yang, C. T. Zhou, and K. A. Tanaka, "Collimation of energetic electrons from a laser-target interaction by a magnetized target back plasma preformed by a long-pulse laser," Phys. Rev. Lett. **112**, 215003 (2014).

[11]A. Poyé, S. Hulin, M. Baillygrandvaux, J. L. Dubois, J. Ribolzi, D. Raffestin, M. Bardon, F. Lubranolavaderci, E. D'Humières, and J. J. Santos, "Physics of giant electromagnetic pulse generation in short-pulse laser experiments," Phys. Rev. E **91**, 043106 (2015).

[12]J. W. Yang, T. S. Li, T. Yi, C. K. Wang, M. Yang, W. M. Yang, S. Y. Liu, S. E. Jiang, and Y. K. Ding, "Measurement and analysis of electromagnetic pulse from laser-target interaction at ShenGuang II laser facility," Fusion Sci. Technol. **72**, 41–48 (2017).

[13]M. Yang, Y. Yang, T. Li, T. Yi, C. Wang, S. Liu, S. Jiang, and Y. Ding, "Electromagnetic radiations from laser interaction with gas-filled Hohlraum," Laser Phys. Lett. **15**, 016101 (2018).

[14]T. Nakamura, S. Kato, H. Nagatomo, and K. Mima, "Surface-magnetic-field and fast-electron current-layer formation by ultraintense laser irradiation," Phys. Rev. Lett. **93**, 265002 (2004).

[15]C. C. Cheng, E. M. Wright, and J. V. Moloney, "Generation of electromagnetic pulses from plasma channels induced by femtosecond light strings," Phys. Rev. Lett. **87**, 213001 (2001).

[16]D. C. Eder, A. Throop, C. G. Brown, J. Kimbrough, Jr., M. L. Stowell, D. A. White, P. Song, N. Back, A. MacPhee, H. Chen, W. DeHope, Y. Ping, B. Maddox, J. Lister, G. Pratt, T. Ma, Y. Tsui, M. Perkins, D. O'Brien, and P. Patel, "Mitigation of electromagnetic pulse (EMP) effects from short-pulse lasers and fusion neutrons," Lawrence Livermore National Laboratory Report No. LLNL-TR-411183, 2009.

[17]J. L. Dubois, F. Lubrano-Lavaderci, D. Raffestin, J. Ribolzi, J. Gazave, A. Compant La Fontaine, E. d'Humieres, S. Hulin, P. Nicolai, A. Poye, and V. T. Tikhonchuk, "Target charging in short-pulse-laser-plasma experiments," Phys. Rev. E **89**, 013102 (2014).

[18]A. Poye, J. L. Dubois, F. Lubrano-Lavaderci, E. D'Humieres, M. Bardon, S. Hulin, M. Bailly-Grandvaux, J. Ribolzi, D. Raffestin, J. J. Santos, P. Nicolai, and V. Tikhonchuk, "Dynamic model of target charging by short laser pulse interactions," Phys. Rev. E **92**, 043107 (2015).

[19]M. J. Mead, D. Neely, J. Gauoin, and R. Heathcote, "Electromagnetic pulse generation within a petawatt laser target chamber," Rev. Sci. Instrum. **75**, 4225–4227 (2004).

[20]C. G. Brown, Jr., J. Ayers, B. Felker, W. Ferguson, J. P. Holder, S. R. Nagel, K. W. Piston, N. Simanovskaia, A. L. Throop, M. Chung, and T. Hilsabeck, "Assessment

and mitigation of diagnostic-generated electromagnetic interference at the National Ignition Facility," Rev. Sci. Instrum. **83**, 10D729 (2012).
[21]J. Li, X. Wang, Z. Chen, J. Zhou, S. S. Mao, and J. Cao, "Real-time probing of ultrafast residual charge dynamics," Appl. Phys. Lett. **98**, 011501 (2011).
[22]C. G. Brown, E. Bond, T. Clancy, S. Dangi, D. C. Eder, W. Ferguson, J. Kimbrough, and A. Throop, "Assessment and mitigation of electromagnetic pulse (EMP) impacts at short-pulse laser facilities," J. Phys.: Conf. Ser. **244**, 032001 (2010).
[23]A. Raven, P. T. Rumsby, J. A. Stamper, O. Willi, R. Illingworth, and R. Thareja, "Dependence of spontaneous magnetic fields in laser produced plasmas on target size and structure," Appl. Phys. Lett. **35**, 526–528 (1979).
[24]M. Manclossi, J. J. Santos, D. Batani, J. Faure, A. Debayle, V. T. Tikhonchuk, and V. Malka, "Study of ultraintense laser-produced fast-electron propagation and filamentation in insulator and metal foil targets by optical emission diagnostics," Phys. Rev. Lett. **96**, 125002 (2006).
[25]F. J. Meng, "Threat of electromagnetic pulse weapon to vehicular photoelectric countermeasure system," OME Inf. **27**(12), 125–129 (2010).
[26]L. Palisek and L. Suchy, in *High Power Microwave Effects on Computer Networks, Sensitive Parts and Comparisons Emc Europe* (IEEE, 2011).
[27]V. A. Chanturiya, I. J. Bunin, and A. T. Kovalev, "Application of high-power electromagnetic pulses to desintegration of gold-containing mineral complexes," in *Pulsed Power Conference* (IEEE, 2005).
[28]G. Inanan, B. Baranoglu, and E. Aydin, "An application of high-power electromagnetic pulse: Forming of sheet metal using electromagnetic waves," in *2015 9th International Conference on Electrical and Electronics Engineering (ELECO)* (IEEE, 2015).
[29]F. Consoli, R. D. Angelis, P. Andreoli, M. Cipriani, G. Cristofari, G. D. Giorgio, and F. Ingenito, "Experiments on electromagnetic pulse (EMP) generated by laser-plasma interaction in nanosecond regime," in *2015 IEEE 15th International Conference on Environment and Electrical Engineering (EEEIC)* (IEEE, 2015).
[30]M. De Marco, J. Krása, J. Cikhardt, A. Velyhan, M. Pfeifer, R. Dudžák, J. Dostál, E. Krouský, J. Limpouch, T. Pisarczyk, Z. Kalinowska, T. Chodukowski, J. Ullschmied, L. Giuffrida, D. Chatain, J. P. Perin, and D. Margarone, "Electromagnetic pulse (EMP) radiation by laser interaction with a solid H_2 ribbon," Phys. Plasmas **24**, 083103 (2017).
[31]J. W. Yang, T. S. Li, T. Yi, C. K. Wang, M. Yang, W. M. Yang, S. Y. Liu, S. E. Jiang, and Y. K. Ding, "Electromagnetic pulses generated from laser target interactions at Shenguang II laser facility," Plasma Sci. Technol. **18**, 1044–1048 (2016).
[32]G. Zhang, L. Hou, Y. Liu, J. Huang, Z. Wang, and R. Ma, "Microwave ignition method based on cylindrical resonant cavity," High Voltage Eng. **42**, 1914–1920 (2016).
[33]G. H. Liu and M. Y. Zhu, "The design of microwave resonator to accurately measure the atmospheric refractivity," Phys. Procedia **33**, 1670–1676 (2012).
[34]H. Ruhl, Y. Sentoku, K. Mima, K. A. Tanaka, and R. Kodama, "Collimated electron jets by intense laser-beam–plasma surface interaction under oblique incidence," Phys. Rev. Lett. **82**, 743–746 (1999).
[35]Y. Sentoku, H. Ruhl, K. Mima, R. Kodama, K. A. Tanaka, and Y. Kishimoto, "Plasma jet formation and magnetic-field generation in the intense laser plasma under oblique incidence," Phys. Plasmas **6**, 2855–2861 (1999).
[36]C. Gahn, G. D. Tsakiris, A. Pukhov, J. Meyertervehn, G. Pretzler, P. Thirolf, D. Habs, and K. J. Witte, "Multi-MeV electron beam generation by direct laser acceleration in high-density plasma channels," Phys. Rev. Lett. **83**, 4772–4775 (1999).
[37]J. P. Freidberg, R. W. Mitchell, R. L. Morse, and L. I. Rudsinski, "Resonant absorption of laser light by plasma targets," Phys. Rev. Lett. **28**, 795–799 (1972).
[38]F. Brunel, "Not-so-resonant, resonant absorption," Phys. Rev. Lett. **59**, 52–55 (1987).
[39]W. L. Kruer and K. Estabrook, "J × B heating by very intense laser light," Phys. Fluids **28**, 430 (1985).
[40]L. M. Chen, J. Zhang, H. Teng, Q. L. Dong, Z. L. Chen, T. J. Liang, L. Z. Zhao, and Z. Y. Wei, "Experimental study of a subpicosecond pulse laser interacting with metallic and dielectric targets," Phys. Rev. E **63**, 036403 (2001).